Advanced Composite Materials
Publication details, including instructions for authors and subscription information:
http://www.tandfonline.com/loi/tacm20

Evaluating the fracture toughness of glass fiber/epoxy interface using slice compression test: propagation behavior of interfacial debonding

K. N. Tsay , K. Toge & H. Kawada

Version of record first published: 02 Apr 2012.

Adv. Composite Mater., Vol. 11, No. 1, pp. 1–9 (2002)

Evaluating the fracture toughness of glass fiber/epoxy interface using slice compression test: propagation behavior of interfacial debonding

K. N. TSAY [1], K. TOGE [2] and H. KAWADA [3]

[1] *Department of Mechanical Engineering, National Taiwan University, Taipei, Taiwan ROC*
[2] *Graduate School of Mechanical Engineering, Waseda University, 3-4-13-4-1 Okubo, Shinjuku, Tokyo 169-8555, Japan*
[3] *Department of Mechanical Engineering, Waseda University, 3-4-1 Okubo, Shinjuku, Tokyo 169-8555, Japan*

Abstract—The slice compression test (SCT) is used to evaluate interfacial properties by loading/unloading a specimen of the composite between two plates; one has low modulus and the other has high modulus. The specimen used is an epoxy resin, containing a single SiO_2 glass fiber, with a 200 μm diameter. The interfacial debonding is monitored by using a microscope and a video camera. Then, the energy release rate is calculated by finite element analysis.

From the *in-situ* observation, it is found that the interface fracture initiates when the radial stress around the fiber changes from compression to tension due to the Poisson's effect (applied stress $\geqslant$40 MPa). The length of the crack is proportional to the stress as the load increases. It is also found analytically that the energy release rates remain constant once the interface fractures, independent of the initial crack length. It is suggested that the critical energy release rate can be appropriated for the interface fracture criterion.

Keywords: Slice compression test; polymeric matrix composites; interfacial debonding; energy release rate.

1. INTRODUCTION

The mechanical performance of a polymer matrix composite (PMC) is closely related to its interfacial properties. To evaluate these interfacial properties, fiber pull-out [1], push-out [2], and push-in [3] tests have been developed. However, these tests can only evaluate a single fiber specimen, and a special indentor and complicated testing machines are required. The slice compression test (SCT) [4–7] can be carried out using a universal testing machine. It involves compressing a polished slice of the composite material which has been cut normally to the fiber between the hard and soft plates. The hard plate has a high modulus and high strength while the soft plate has a low modulus and a low yield stress. Up to a certain load, the fiber–matrix interface initially debonds, the crack grows and finally fibers protrude, making permanent imprints on the soft plate. When the loading is released, the fibers at the bottom surface partially relax back into the matrix and retain residual protrusion. Kagawa and Honda [8], Hsueh [4, 5], and Shafry and Brandon [6, 7] have done theoretical and experimental studies concerning SCT for a ceramic-matrix composite.

The SCT was originally developed to evaluate the interfacial properties of ceramic-matrix based composites. It has seldom been applied to the PMC. Furthermore, no failure criterion for the interface debonding by the use of the SCT is available. One of the authors [9] first applied the slice compression test to PMC. They tried to develop a stress-based failure criterion for the slice compression test. However, the singularity of the stress field near the crack tip makes it difficult to evaluate the interfacial properties.

In this paper, the SCT is also applied to a polymer matrix composite. The progressive debonding process is observed using a circular polariscope. By observing the development of photoelastic fringes in the matrix, the debond length can be accurately measured and correlated to the loading stress. A numerical analysis is carried out to identify the stress field before, upon and after the initial debonding occurs. In the current work, finite element analysis is also performed to calculate the energy release rate for the interface fracture criterion.

2. EXPERIMENTAL PROCEDURE

2.1. Materials and specimen preparation

Epicote 828 was used as the matrix, containing a single glass fiber (SiO_2) with a 200 μm diameter (Fig. 1). The curing temperature was 373 K with a heating rate of 1 K min^{-1}. The material properties of the constituents are listed in Table 1. The specimens were then cut normal to the fiber direction, thickness 6 ± 0.5 mm, and both surfaces were polished up to 1 μm with a diamond paste. However, most of the interfaces between the fiber and the matrix were debonded near the surface after being polished.

Table 1.
Material properties of constituents

	SiO_2	SiC	Epoxy
E (GPa)	78	406	3.0
ν	0.14	0.15	0.37
α_z (10^{-6}/K)	0.5	5	65
α_r (10^{-6}/K)	0.5	2.63	65

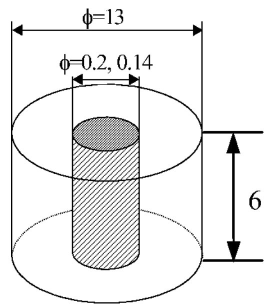

Figure 1. Illustration of specimen geometry.

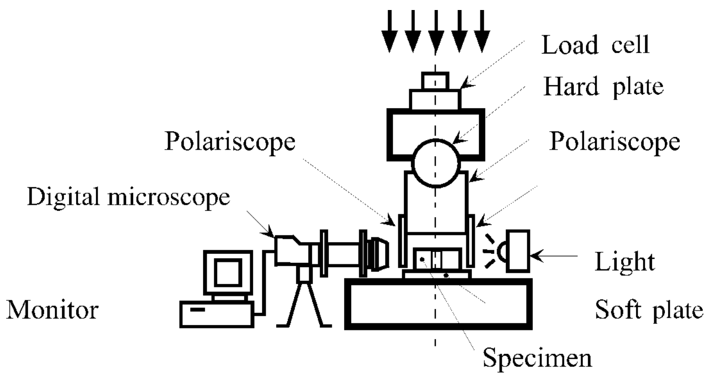

Figure 2. Schematic drawing of SCT.

2.2. Measurements

The SCT was carried out at room temperature using a standard compression testing machine. The specimen was located parallel to the loading direction and sandwiched between the soft plate, annealed Al1050 (thickness: 3 mm, $E = 60$ MPa, initial yield stress $\risingdotseq 10$ MPa), and the hard plate, SUS303($E = 193$ GPa, initial yield stress $\risingdotseq 689$ MPa). A relatively slow rate of compression, 0.05 mm/min, was employed. The microscopic images were transferred to the recorder and displayed on a monitor (Fig. 2). The specimens were transparent because of the epoxy matrix. The tip of the interfacial debonding could be traced under the appropriate reflection of the light and the corresponding debonded length could be determined on the LCD monitor directly.

3. EXPERIMENTAL RESULTS

It has been observed that a crack initiated near the soft plate and propagated along the SiO_2 fiber/epoxy matrix interface. The crack growth was monitored using a digital microscope and a recorder when the applied load was increased continuously, as presented in Fig. 3. Relative debonding lengths are plotted in Fig. 4 as a function of the compressive applied stress. The relative debonding lengths distribute into two main lines owing to the different initial debonding lengths. There is no apparent crack propagation when the load is under 40 MPa. The crack propagation initiates when the load is over 40 MPa; so we can infer that the interfacial stress distribution changed when the load was over 40 MPa.

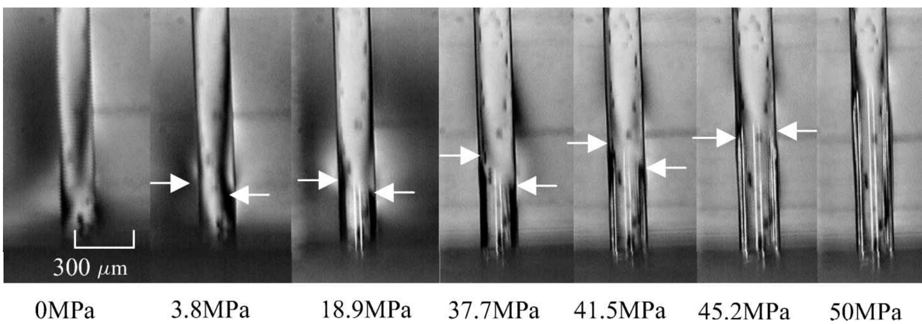

Figure 3. Interfacial debonding propagation.

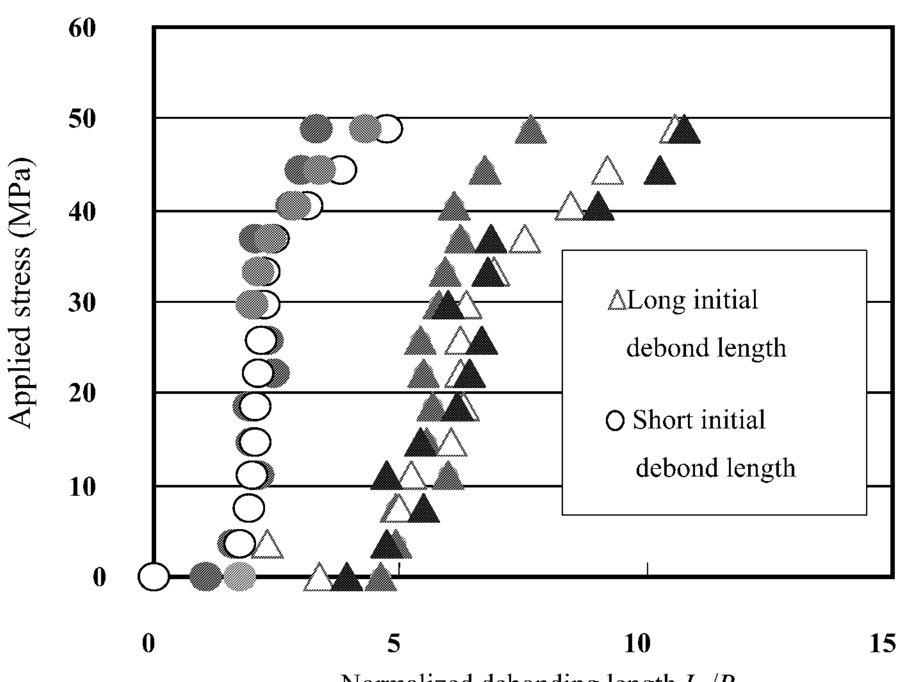

Figure 4. Relation between applied stress and debonding length.

4. ANALYSIS AND DISCUSSION

To analyze the interfacial stress distribution when the specimen is stressed, a composite-cylinder model is adopted (Fig. 5) to simplify the problem. In this case, the radial stress is the main factor that affects the debonding process. There are two sources of radial stress at the interface of the composite: (1) residual clamping stress σ_c which is due to the mismatch of the thermal expansion of the coefficient during cooling from the curing temperature when the thermal expansion coefficient of the matrix is higher than the fiber and (2) the stress σ_p which is due to the Poisson's expansion of the specimen in the radial direction when the specimen is subjected to axial compressive stress.

The radial stress σ_p can be related to loading stress σ as follows [4]:

$$\sigma_p = \frac{\left(\dfrac{\nu_f E_m}{E_f} + \dfrac{a^2 \nu_m}{b^2 - a^2}\right)\sigma_f - \dfrac{b^2 \nu_m \sigma}{b^2 - a^2}}{D}, \tag{1}$$

where E and ν are Young's modulus and Poisson's ratio, and the subscripts, f and m, show the fiber and the matrix, respectively.

D is given as

$$D = \frac{b^2 + a^2}{b^2 - a^2} + \nu_m + \frac{(1 - \nu_f)E_m}{E_f}. \tag{2}$$

The clamping stress σ_c is derived by [10]

$$\begin{aligned}\sigma_c = A\Bigg[&\left(\frac{1+\nu_f}{E_f} + \frac{f}{1-f}\frac{1+\nu_m}{E_m}\right)\alpha_m - \left(\frac{1}{E_f} + \frac{f}{(1-f)E_m}\right)\alpha_f \\ &- \left(\frac{\nu_f}{E_f} + \frac{f\nu_m}{(1-f)E_m}\right)\alpha_z\Bigg]\Delta T,\end{aligned} \tag{3}$$

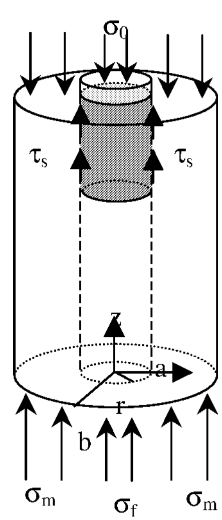

Figure 5. Composite cylinder model for SCT analysis.

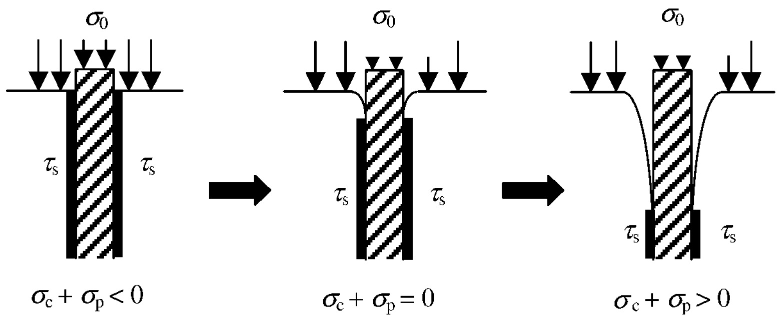

Figure 6. Debonding process of PMC with SCT.

where α is the coefficient of thermal expansion, the subscripts z denote the axial direction of the specimen, f is the fiber volume fraction, and ΔT is a change in the temperature.

A is given as follows:

$$A = \left\{ \frac{(1+\nu_f)(1-2\nu_f)}{E_f^2} + \frac{f(2-\nu_f-\nu_m-4\nu_f\nu_m)+1+\nu_m}{(1-f)E_fE_m} + \frac{f(1+\nu_m)(1+f-2f\nu_m)}{(1-f)^2E_m^2} \right\}^{-1}. \tag{4}$$

The interfacial debonding and sliding process of the PMC interface using SCT is schematically shown in Fig. 6. Before loading, only the residual clamping stress closes the interface. The effect from the stress induced by the Poisson's effect increased with the applied stress. Finally, the contact between the fiber and the matrix vanishes at the specimen's surface when the load reaches the critical value. When $\sigma_p + \sigma_c = 0$, the interface starts opening and the applied stress at this time is calculated by equation (1) = equation (3) which is 44.3 MPa. Thus, the experimental result can be explained by the crack propagation which initiates when the applied stress is about 40 MPa.

5. FINITE ELEMENT ANALYSIS

5.1. Finite element model

The FE analysis was carried out using an axisymmetric mesh (Fig. 7) with eight-noded elements and linear-elastic material properties. The stress-intensity factor was calculated by the extrapolation method. The energy release rate was obtained from the FE results by the relationship between the energy release rate and the stress-intensity factors for bimaterial cracks [11]:

$$G = \frac{1}{4\cosh^2(\varepsilon\pi)} \left\{ \frac{1-\nu_f}{G_f} + \frac{1-\nu_m}{G_m} \right\} \left(K_1^2 + K_2^2\right), \tag{5}$$

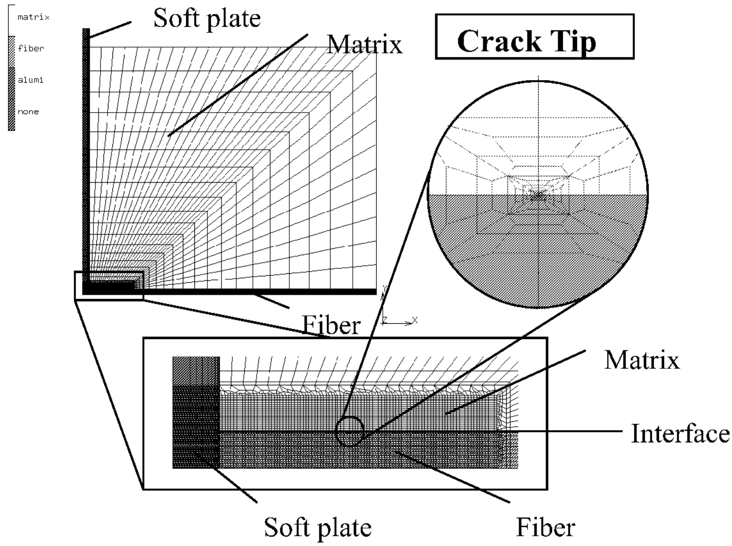

Figure 7. Finite element model.

where G_f and G_m are the fiber and matrix shear modulus, and ε is a bimaterial constant. Equation (5) is strictly valid in plane-strain conditions, which are a good approximation for the interface region in an axisymmetric model, provided that at least the fiber is rigid compared to the matrix; this was expressed [12] in the results of the FE analysis.

5.2. Finite element results for energy release rate

The relationship between the debonding length and the energy release rate are presented in the FE results (Fig. 8) using equation (5) and the stress-intensity factor calculated from the experimental result (Fig. 4). An interesting region can be found in the range of medium crack lengths in both the initial crack length conditions, where the energy release rate itself shows only a slight change in this range, denoted also as a ‘plateau range’ in this paper. To evaluate the debonding process of the PMC composite, a critical energy release rate can be defined as a criterion.

6. CONCLUSIONS

(1) The slice compression test is used to evaluate the interfacial debonding process of the SiO_2/epoxy composite. The obtained applied stress that opens the interface is compared to the results proposed by our group [9], the relation of the fiber protrusion and the loading stress, on the same system. There is good agreement between the two viewpoints.

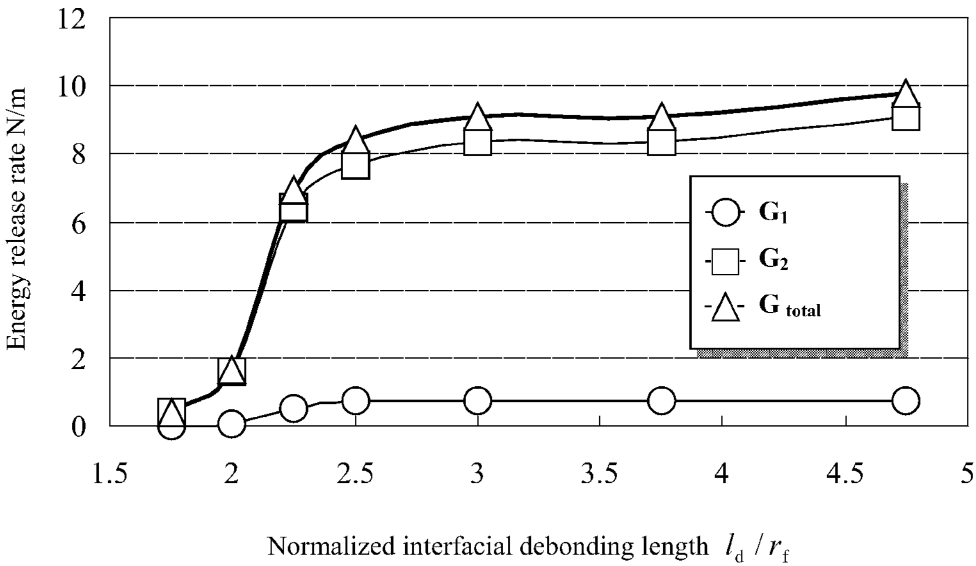

Figure 8. Dependence of energy release rate on debonding length.

(2) The interfacial debonding proceeds after the interface opening, when the compressive loading stress overcomes a particular value because of the Poisson effect.

(3) The critical energy release rate can be defined to be able to evaluate the interfacial debonding propagation in both the lengths of the initial debonding.

REFERENCES

1. J. P. Favre, Advances in pull-out testing and data analysis, *Compos. Sci. Technol.* **42**, 151–187 (1991).
2. A. F. Kalton, C. M. Wrad-Close and T. W. Clyne, Development of the tensioned push-out test for study of fibre/matrix interfaces, *Composites* **25**, 637–644 (1994).
3. D. B. Marshall, *Acta Metall. Mater.* **40** (3), 427–441 (1992).
4. C. H. Hsueh, Analyses of slice compression tests for aligned ceramic matrix composites, *Acta Metall. Mater.* **41** (12), 3585–3593 (1993).
5. C. H. Hsueh, Slice compression tests versus fiber push-in tests, *J. Compos. Mater.* **28** (7), 638–655 (1994).
6. N. Shafry, D. G. Brandon and M. Terasaki, *Euro Ceramics* **3**, 3453 (1989).
7. C. H. Hsueh, D. G. Brandon and N. Shafry, Experimental and theoretical aspects of slice compression tests, *Mater. Sci. Engng.* **A205**, 91–100 (1996).
8. Y. Kagawa and K. Honda, *Ceram. Eng. Sci. Proc.* **12** (7–8), 1127–1138 (1991).
9. N. Taniguchi, K. Toge and H. Kawada, Evaluation of the mechanical properties of PMC interface using slice compression test, *Composite Interfaces* 2000 Proceedings.
10. C. H. Hsueh and P. F. Becher, *J. Am. Ceram. Soc.* **71**, C438 (1988).
11. J. R. Rice, Elastic fracture mechanics concepts for interfacial cracks, *J. Appl. Mech.* **55**, 98–103 (1988).

12. C. Atkinson, J. Avila, E. Betz and R. E. Smelser, The rod pull out problem, theory and experiment, *J. Mech. Phys. Solids* **30**, 97–120 (1982).
13. R. S. Dhaliwal, H. S. Saxena, W. He and J. G. Rokne, Stress intensity factor for the cylindrical interface crack between nonhomogeneous coaxial finite elastic cylinders, *Engineering Fracture Mechanics* **43**, 6 (1992).